


Article

Whole-Cell PVA Cryogel-Immobilized Microbial Consortium LE-C1 for Xanthan Depolymerization

Elena V. Zhurishkina ^{1,2}, Elena V. Eneyskaya ^{1,2}, Svetlana V. Shvetsova ^{1,2}, Lyudmila V. Yurchenko ¹, Kirill S. Bobrov ^{1,2} and Anna A. Kulminskaya ^{1,2,*} 

¹ Petersburg Nuclear Physics Institute Named by B.P. Konstantinov of National Research Center “Kurchatov Institute”, 1, mkr. Orlova roshcha, Gatchina 188300, Russia

² Kurchatov Genome Center—PNPI, 1, mkr. Orlova roshcha, Gatchina 188300, Russia

* Correspondence: kulminskaya_aa@pnpi.nrcki.ru; Tel.: +7-(81371)-32014

Abstract: Xanthan is an extracellular heteropolysaccharide produced by the bacteria *Xanthomonas campestris*. Due to its unique properties, the polysaccharide and its derivatives are widely used in many industries, from food to biomedicine and oil production, that demands an efficient xanthan depolymerization method to adapt this polysaccharide for various applications. Unlike the known chemical approaches, biological methods are considered to be more environmentally friendly and less energy intensive. In laboratory conditions, we have isolated a bacterial community capable of reducing the xanthan viscosity. Identification of the individual isolates in the microbial community and their testing resulted in the consortium LE-C1, consisting of two microorganisms *Paenibacillus phytohabitans* KG5 and *Cellulosimicrobium cellulans* KG3. The specific activities of the overall xanthanase and auxiliary enzymes that may be involved in the xanthan depolymerization were as follows: xanthanase, 19.6 ± 0.6 U/g; β -glucosidase, 3.4 ± 0.1 U/g; α -mannosidase, 68.0 ± 2.0 U/g; β -mannosidase, 0.40 ± 0.01 U/g; endo-glucanase, 4.0 ± 0.1 U/g; and xanthan lyase, 2.20 ± 0.07 U/mg. In order to increase the efficiency of xanthan biodegradation, the LE-C1 whole cells were immobilized in a poly(vinyl alcohol) cryogel. The resulting regenerative biocatalyst was able to complete xanthan depolymerization within 40 cycles without loss of activity or degradation of the matrix.

Keywords: xanthan; xanthanase; biodegradation; enzymes activities; microbial consortium; cell immobilization; polyvinyl alcohol; regenerable biocatalyst



Citation: Zhurishkina, E.V.; Eneyskaya, E.V.; Shvetsova, S.V.; Yurchenko, L.V.; Bobrov, K.S.; Kulminskaya, A.A. Whole-Cell PVA Cryogel-Immobilized Microbial Consortium LE-C1 for Xanthan Depolymerization. *Catalysts* **2023**, *13*, 1249. <https://doi.org/10.3390/catal13091249>

Academic Editors: Wei Du, Sulaiman Al-Zuhair and Miao Guo

Received: 13 July 2023

Revised: 14 August 2023

Accepted: 24 August 2023

Published: 29 August 2023



Copyright: © 2023 by the authors. Licensee MDPI, Basel, Switzerland. This article is an open access article distributed under the terms and conditions of the Creative Commons Attribution (CC BY) license (<https://creativecommons.org/licenses/by/4.0/>).

1. Introduction

Xanthan is an extracellular heteropolysaccharide produced by many strains of the bacteria *Xanthomonas* [1,2]. The main xanthan chain consists of D-glucopyranose residues linked by a β -1,4-glycosidic bond, where every second glucose residue is linked by a (3→1)-bond to the α -D-Man-(2→1) β -D-GlcA(4→1)- β -D-Man [2–5]. The side chains of xanthan are modified with pyruvate and/or acetate groups leading to a higher reactivity and hydrophilicity, as well as the ability to form complexes when compared to other polysaccharides [6–8].

Due to its properties, xanthan gum is widely used in various fields: food, pharmaceutical, cosmetic, agriculture, oil production, and paint and varnish industries as a thickener, stabilizer, or suspending agent [9–12]. Various methods are now being developed for the use of xanthan and its derivatives in biomedicine [12–17]. A large amount of xanthan gum is used in oil production as a drilling fluid structurant to increase the viscosity of the fluids in order to prevent the well from collapsing [18]. In oil production, at the end of the work, the question of how to dispose the used drilling fluid in an environmentally friendly manner is acute. Thus, many studies are demonstrating a growing interest in developing approaches for efficient xanthan depolymerization in order to adapt this polysaccharide for applications in many areas.

Traditional xanthan depolymerization methods are chemical hydrolysis with strong acids and high temperatures [19]. As an alternative, biological methods are considered more environmentally friendly and less energy consuming by using microorganisms or enzyme mixtures [9]. Based on the xanthan structure, the depolymerization requires the presence of an enzyme complex. Presumably, such a complex may include xanthan lyase, endo- β -D-glucanase, β -D-glucosidase, α -/ β -mannosidases, and acetyl esterase, which are the most frequently mentioned enzymes in the “xanthanase complex”, or the term used in a general sense “xanthanase” [9]. A search for new enzymes is currently underway as well as testing previously characterized enzymes or their combinations: cellobiohydrolase, endo-xanthanase, and unsaturated glucuronyl hydrolase [20–23]. To the best of our knowledge, xanthan-degrading microorganisms are poorly represented in the scientific literature. The genes encoding the required set of enzymes are mainly described in bacteria. Among the producers of enzymes of the xanthan-degrading complex, bacteria of the genera *Bacillus*, *Paenibacillus*, *Cellulomonas*, and *Microbacterium* are most often described: *Bacillus* sp. GL1, *Paenibacillus xanthanilyticus* sp. nov., and *Paenibacillus* sp. XD [23–31]. Among fungal microorganisms, strains of *Chaetomium globosum* CGMCC 6882 and *Myceliophthora thermophila* C1 have been reported [32,33]. A single bacterium species is rarely characterized by the presence of a set of enzymes capable of the complete destruction of xanthan main and side chains. More often, bacterial consortia and mixed cultures capable of total xanthan degradation have been reported [34,35]. Thus, the identification of new microorganisms that are efficient at xanthan degradation is still required.

Whole-cell biocatalysts based on the physical restriction of cells in a certain area of space lead to efficient bioconversion of complex substrates [36]. Microbial cell immobilization technologies have existed for many decades and have been widely used in various processes, such as wastewater treatment, environmental remediation, biodegradation, chemical analysis, food processing, energy development, medicine and pharmaceuticals, and other fields [36–39]. For each process, an individual choice of a biocatalyst, matrix, immobilization conditions, and spatial distribution in the matrix structure is required, which should ensure the duration of the process and its repeated usage without loss of activity and stability [40]. The improvement in the efficiency of xanthan degradation for various practical applications can be reached by creating a microbial system based on immobilized microbial cells with targeted functions.

Here, we present characteristics of a new microbial consortium for the efficient depolymerization of xanthan. On the basis of two genetically identified individual strains isolated from a bacterial community grown on a xanthan-containing medium, a biocatalyst with microbial cells immobilized within a polyvinyl alcohol matrix was developed for the stable degradation of the complexed polysaccharide.

2. Results and Discussion

2.1. Screening, Isolation, and Identification of Xanthan-Degrading Microorganisms

For screening of xanthan-degrading microorganisms, a 0.3% solution of xanthan gum was poured into 15 test tubes and kept outdoors in a laboratory for 14 days. The reduction in viscosity of the tube contents was used as an indication of xanthan-degrading activity. In three of these test tubes, the growth of microorganisms and a decrease in the viscosity of the initial solution were observed. During the 8-day growth of the microbial preparation with the highest xanthan-degrading potential, the viscosity of the XP medium reduced from 250 cPs to a water viscosity value. Monitoring the changes in the amount of reducing sugars in the culture liquid of this particular microbial community resulted in a bell-shaped curve with a maximum on the 4th day and a decline by the end of the 8th day of growth (Figure 1).

Microscopic examination of the preparation with the highest potential revealed a microbial community containing several species. Enrichment of this community by several passages on solid XP and LB media at 28 °C for 1–3 days resulted in the final natural consortium LE-C1 consisting of only two microorganisms with xanthan-depolymerizing

abilities, KG3 and KG5. Therefore, the final bacterial mix LE-C1 and individual isolates KG3 and KG5 were taken for further studies.

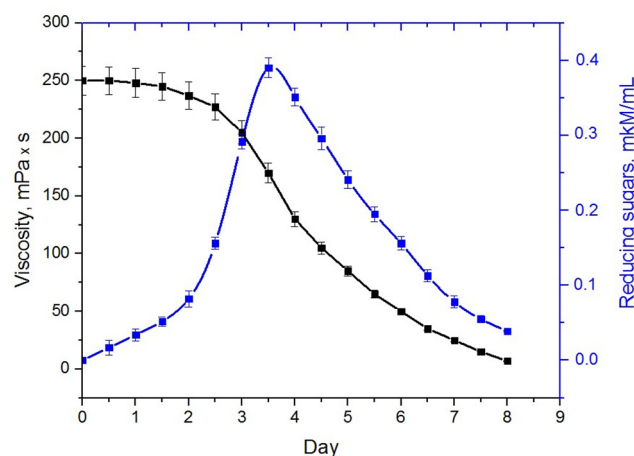


Figure 1. Time course of xanthan depolymerization from the microbial preparation with the highest potential during the growth in a liquid XP medium. Samples were taken and assayed for cell viscosity and changes in reducing sugars. Viscosity (black line) was measured with an LVF Brookfield viscosimeter at 22 °C. Reducing sugars (blue line) were assayed by the method [41]. Bars indicate standard errors.

Morphological analysis of the individual strains revealed the following features of each of the isolates.

An isolate of KG3: Vegetative cells were immobile twisted Gram-positive rods 0.3–0.6 × 4–5.0 µm in size transforming into coccobacilli during prolonged incubation. On LB medium, bacterial cells formed a dull-white, shiny, bumpy colonies with smooth edges, which eventually turned yellow.

An isolate of KG5: The vegetative cells were mostly single Gram-positive rods 1.0 × 4–6.0 µm in size. The cells produced oval spores located terminally in swelling sporangia. On LB medium, bacterial cells formed transparent, colorless, convex or slightly flattened, shiny colonies with smooth edges.

Genomic DNA samples were isolated from the culture broths and the 16S rDNA sequences of both selected strains were compared to those available in the BLASTN database. The phylogenetic trees were constructed with the maximum likelihood and Tamura-Nei model [42] as shown in Figure 2.

Based on the morphological features and genetic analysis, the strains KG3 and KG5 were identified as *Cellulosimicrobium cellulans* KG3 and *Paenibacillus phytohabitans* KG5, respectively. Both strains were deposited at the National Bioresource Center “All-Russian Collection of Industrial Microorganisms” under the numbers AC-2213 and B-14516, correspondingly.

2.2. Characterization of Xanthan-Degrading Activity

The xanthan liquefaction capacity for each of the isolates was studied in detail during their growth in a liquid XP medium. *P. phytohabitans* KG5 completely reduced the viscosity of the xanthan solution within 72 h (Figure 3a), which is 2.5 times faster than was observed with the original microbial community (Figure 1). The *C. cellulans* KG3 strain reduced the viscosity by 25% of the initial value during the first 30 h of cultivation and then the viscosity level remained unchanged throughout the entire observation period (Figure 3a). Mixing the two cultures at a 1:1 ratio led to a complete xanthan depolymerization after 48 h, which was noticeably more effective than for the most active *P. phytohabitans* KG5 strain (Figure 3a). During a decrease in the xanthan viscosity, we observed an accumulation of reducing ends and the formation of low molecular weight reaction products (Figure 3b).

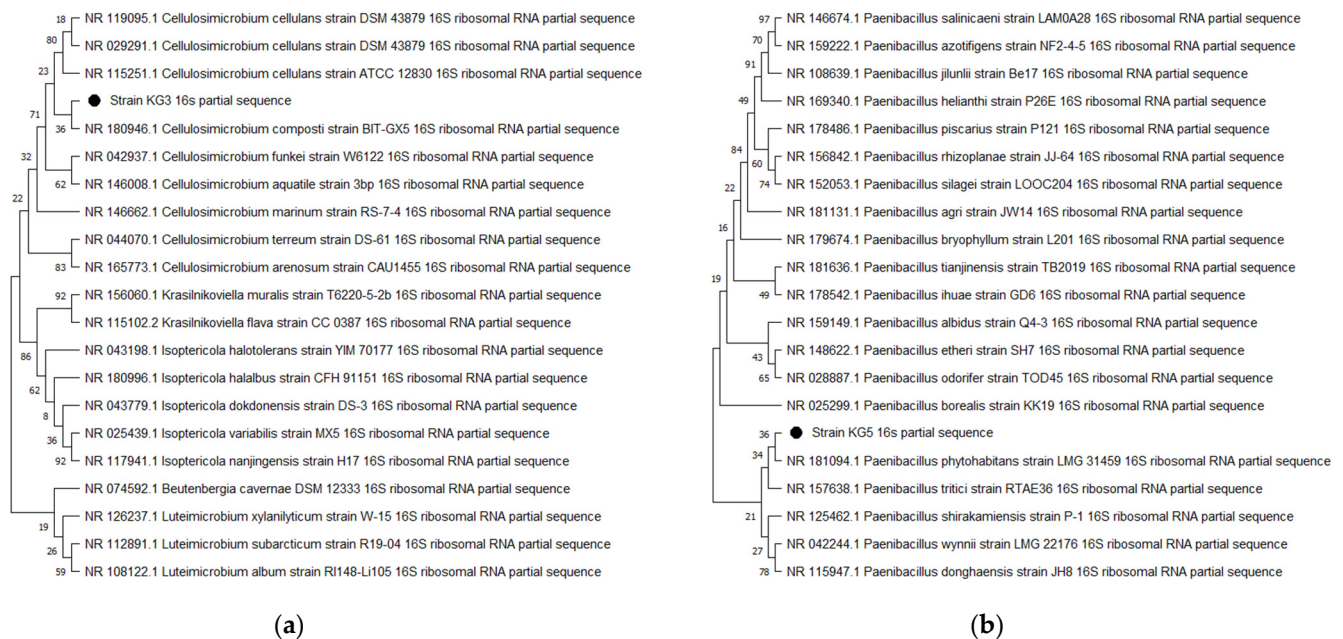
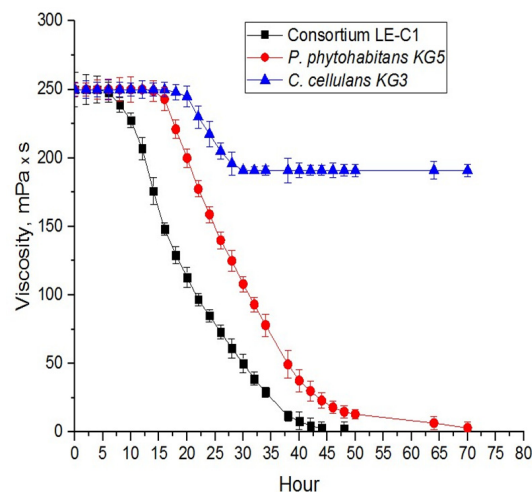
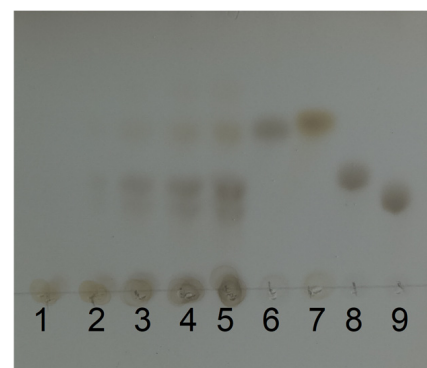


Figure 2. Phylogenetic trees constructed for the selected strains of KG3 and KG5 are based on 16S rRNA gene sequences. The trees with the highest log likelihood (-4296.27 (a); -5204.00 (b)) are shown. The percentage of trees in which the associated taxa clustered together is shown next to the branches. Initial tree(s) for the heuristic search were obtained automatically by applying Neighbor-Join and BioNJ algorithms to a matrix of pairwise distances estimated using the Tamura-Nei model and then selecting the topology with the superior log likelihood value. This analysis involved 21 nucleotide sequences. There were a total of 1535 (a) and 1563 (b) positions in the final dataset. Evolutionary analyses were conducted in MEGA X [43].



(a)



(b)

Figure 3. Xanthan depolymerization analysis during the growth of *C. cellulans* KG3, *P. phytohabitans* KG5, and the consortium LE-C1. Both microorganisms and the consortium LE-C1 have been cultivated in 100 mL of XP medium in Erlenmeyer flasks at 28°C with aeration. Aliquots were withdrawn periodically and viscosity (a) was measured with an LVF Brookfield viscosimeter at 25°C . Bars indicate standard errors. (b) TLC analysis of xanthan depolymerization products during the growth of the consortium LE-C1 was carried out at 0 h (lane 1), 10 h (lane 2), 18 h (lane 3), 28 h (lane 4), and 35 h (lane 5); sugar standards: glucose (lane 6), mannose (lane 7), cellotriose (lane 8), and cellotetraose (lane 9).

To determine the optimal conditions for xanthanase activity produced by the consortium LE-C1 and its stability, a range of different pH values (Figure 4a) and temperatures (Figure 4b) were used. The maximum overall xanthanase activity was detected in the pH range from pH 5.5 to 6.0 and at 40 °C. The xanthanase activity was stable in the pH range from 5.5 to 7 and retained more than 60% of the activity at 45 °C for 15 min (Figure 4b).

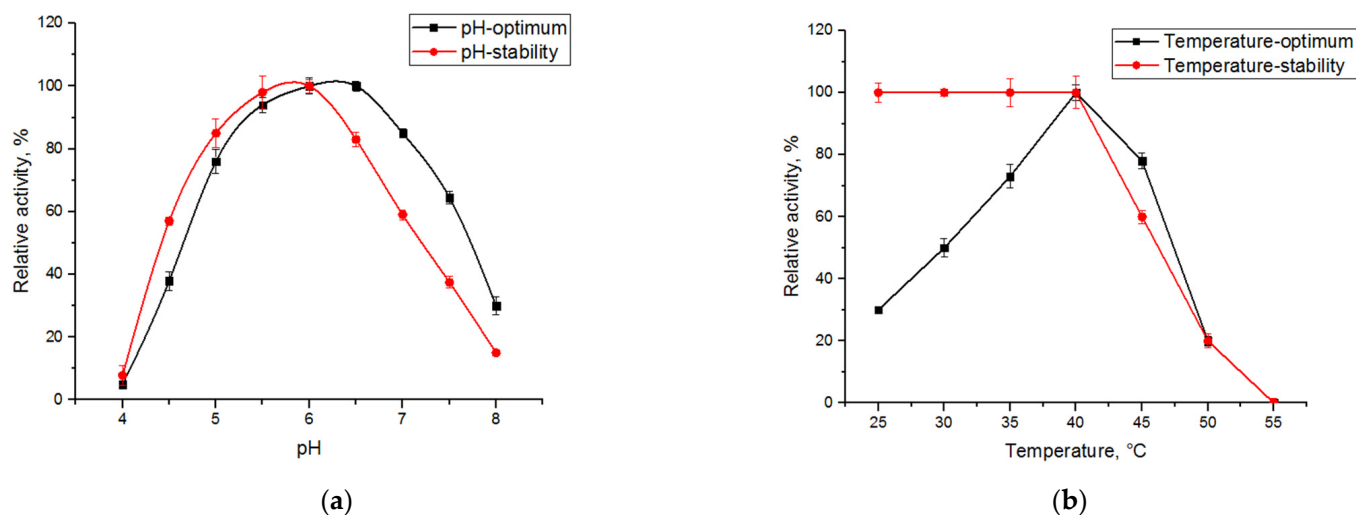


Figure 4. Effects of pH and temperature on the xanthanase activity and stability of the enzyme complex produced by the LE-C1 consortium. Xanthanase activity was measured following the accumulation of reducing sugars by the method [41]. To determine the optimal pH ((a) panel, black line), xanthanase activity was assayed using citrate–phosphate (pH 3.0–7.6) and Tris-HCl (pH 8.0–9.0) buffer solutions at 40 °C. To check the pH stability ((a) panel, red line), the samples were preincubated at various pH values (pH 3.0–9.0) at room temperature for 24 h followed by a standard activity assay. To determine the optimum xanthanase temperature, enzyme activity was measured at various temperatures (4 °C, 25–60 °C) and pH 6.0 ((b) panel, black line). Thermostability of the consortium xanthanase was evaluated after preincubation of the liquid broth samples at various temperatures and pH 6.0 for 15 min ((b) panel, red line). The highest values were taken as 100%.

Comparison of the specific activities assayed after the growth of *P. phytohabitans* KG5 and *C. cellulans* KG3 and their consortium LE-C1 in XP medium revealed the different impacts of the particular enzymes of each microorganism in the overall xanthan-depolymerizing ability of the consortium (Table 1). These results were somewhat surprising because along with the overall positive effect of the LE-C1 consortium on xanthan depolymerization (Figure 3a), we observed a noticeable decrease in the specific enzyme activities of the *C. cellulans* KG3 strain in the consortium compared to its individual growth in XP medium (Table 1). This can be explained by different sets of enzymes synthesized by each microorganism in the mix that regulate the action of each component.

Table 1. Specific enzyme activities in the xanthanase complex of the LE-C1 consortium and its components.

Microorganism(s)	Specific Activity *					
	Xanthanase, U/g	Xanthan Lyase, U/g	β -Glucosidase, U/g	Endo-Glucanase/ Cellobiohydrolase, U/g	α -Mannosidase, U/g	β -Mannosidase, U/g
LE-C1	19.6 \pm 0.6	2200 \pm 70	3.4 \pm 0.1	4.0 \pm 0.1	68.0 \pm 2.0	0.40 \pm 0.01
<i>P. phytohabitans</i> KG5	19.3 \pm 0.6	1660 \pm 50	n.d.	n.d.	n.d.	n.d.
<i>C. cellulans</i> KG3	n.d.	n.d.	80.0 \pm 2.4	30.0 \pm 0.9	130.0 \pm 3.9	70.0 \pm 2.1

* Specific activities were assayed using the corresponding substrate and method as described in Materials and Methods section. n.d., not detected. Data are the means of three experiments \pm standard errors.

Representatives of the genus *Paenibacillus* have been reported to exhibit xanthan-degrading activities due to their production of xanthan lyases [28,29,44,45]. On the other hand, representatives of the genus *Cellulosimicrobium* are potentially capable of hydrolyzing the main and side chains of the xanthan due to the action of various glycoside hydrolases found [46,47]; in particular, due to the presence of cellulases and hemicellulases identified in the genome of *C. cellulans* [48]. However, for their action, xanthan should be in a highly disordered conformation [49].

We assumed that a xanthan lyase, secreted by the *P. phytohabitans* KG5 strain, promoted the cleavage of terminated pyruvated mannosyl and glucuronyl residues in the xanthan side chains. This leads to a conformation disorder in the native xanthan molecule and, as such, facilitates the actions of mannosidases and cellulases, secreted by the *C. cellulans* KG3, which catalyzes the hydrolysis of the rest of trisaccharide side backbones and the core part leading to the intensive accumulation of glucose. Glucose is known to inhibit the expression of most glycoside hydrolases [50] providing a decrease in the overall level of cellulase and hemicellulase activities. In an individual culture of *C. cellulans* KG3, complete hydrolysis of xanthan does not occur due to lack of the necessary xanthan lyase; therefore, glucose is not rapidly accumulated in amounts required to suppress the expression of hemicellulase and cellulase genes. However, this assumption can be checked after detailed proteomic and transcriptomic studies of both individual cultures and their actions in this consortium, which may be a task for future research. Our data confirms that mixing two bacterial cultures resulted in higher efficiency of the consortium vs. individual strains. Similar effects for mixed cultures have been shown earlier [35].

2.3. Immobilization of the LE-C1 Consortium

To immobilize a consortium of LE-C1 cells, zeolite granules, alginate microcapsules, and a polyvinyl alcohol cryogel were tested (Figure 5). Here, we used the LE-C1 consortium that combined the individual strains KG3 and KG5 in a 1:1 ratio. Preliminary tests of the xanthanase activity in both initial and artificial consortia revealed no differences.

Zeolites have been widely used as materials for bacteria immobilization in wastewater treatment processes due to their wide distribution in nature, availability and feasibility, cost-effectiveness, large specific surface area, structural rigidity, surface functionality, and thermal, mechanical, and radiation stability [51–53]. Many factors have been described to be responsible for cell adhesion to inert surfaces. The pore size of the matrix has been considered the most important factor, having a greater effect than macroscopic surface roughness and total surface area [53,54].

For immobilization of the LE-C1 consortium, zeolite (choline zeolite) granules of different sizes were used: 0–1 mm; 1–3 mm; or 3–5 mm (Figure 5a). In the first cycle, the rates of xanthan depolymerization were comparable to samples with zeolite granules with sizes of 1–3 mm and 3–5 mm; in the second cycle, the activity of the sample with 1–3 mm granules was significantly reduced; and in the third cycle, only the sample using 0–1 mm pellets was active. Thus, granules with the smallest size (0–1 mm) appeared to be the most suitable for immobilization. However, we found that cells were leaching from the zeolite matrix during its functioning due to their weak binding resulting in no more than three cycles of the xanthan degradation (Figure 5d, black curve). Thus, further use of zeolite granules for xanthan liquefaction was concluded to be inappropriate due to the decrease and further reduction in the xanthan biodegradation rate during testing.

The system with calcium alginate is widely used for bioimmobilization since the conditions for inclusion in the calcium alginate gel are very mild, the polymer can be sterilized by autoclaving, and the immobilization process is reversible due to the addition of a binding Ca^{2+} reagent (e.g., EDTA or citric acid) [55]. Cells of the LE-C1 consortium immobilized in alginate microcapsules appeared to be active in xanthan degradation during three cycles (Figure 5b,d, red curve). However, after the 4th cycle, the microcapsules acquired a loose structure, presumably, under the influence of enzymes secreted by the bacteria, and were considered to be unsuitable for further work.

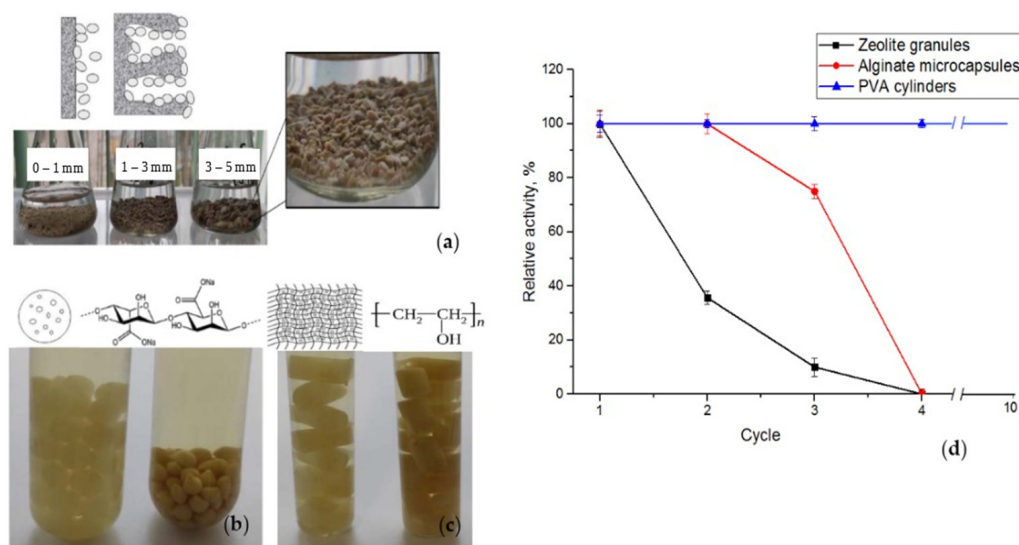


Figure 5. Immobilization of LE-C1 consortium cells by three techniques. (a): immobilized cells of the LE-C1 consortium by adsorption on zeolites with granule sizes of 0–1 mm, 1–3 mm, 3–5 mm. (b): alginate beads with immobilized LE-C1 cells (freshly prepared microcapsules are shown on the left and after four working cycles on the right). (c): immobilized LE-C1 cells in a PVA cryogel (left: freshly prepared cylinders and right: after 10 working cycles). (d): working capacity of biocatalysts: the number of working cycles for the LE-C1 consortium immobilized by adsorption on zeolite granules 0–1 mm in size (black line), in alginate microcapsules (red line), and in PVA cryogel (blue line). The activity of the catalyst in the 1st cycle was taken as 100%.

Cryogels were first described in 1972 (reviewed by Lozinsky [56]). Since that time, they have been quite well-studied and widely used in many biomedical and biotechnological applications [57]. PVA cryogels are formed during the cryogenic cycle (freezing–storage in a frozen state–thawing) with solutions of this polymer. During the process of cryogelation in an aqueous medium, regions are formed where the dissolved polymer is concentrated and undergoes crosslinking reactions [58]. The formation of a chemically stable cryogel occurs due to multiple intermolecular hydrogen bonds between polymer chains resulting from the freezing of the solvent (aqueous phase) and keeping the polymer chains in a frozen state in a relatively immobile state relative to each other. At the initial stage of solution freezing, the crystals formed during the freezing of the solvent will grow and come into contact with neighboring crystals forming a labyrinthine system of interconnected channels (pores) after the sample is thawed. So that the growing ice crystals act as a porogen determining the shape and size of the pores formed after the sample is thawed.

The unique porous structure of poly(vinyl) alcohol (PVA) cryogels, combined with their elasticity and high mechanical stability, the availability of PVA, and biocompatibility, have led to their widespread use as matrices for immobilizing microbial cells (reviewed by Plieva et al. [59]). Depending on the pore size of the cryogels and the potential application of immobilized cellular biocatalysts, immobilization by mechanical entrapment in cryogels or the use of specific ligands to bind cells on the pore surface is used. Preparation of a bacterial cell suspension in a polymer solution for inclusion in its pores (mechanical entrapment) is the simplest and an inexpensive process. Immobilization of bacterial cells in the PVA cryogel matrix leads to their spatial distribution throughout the carrier space keeping cells in a metabolically active state at a certain distance from each other. This prevents their aggregation and the deterioration of conditions for mass transfer processes that increase the efficiency of xanthan biodegradation and leads to multiple uses for the biocatalyst. Cells of the LE-C1 mix immobilized with a 12% solution of PVA showed the highest functioning productivity during 10 cycles without any loss of the overall xanthanase activity (Figure 5a,d, blue line).

Summarizing the above data, we found that immobilized cells in alginate or PVA showed higher activity compared to the zeolite carriers that might be explained by the maintenance of a constant number of cells due to stronger binding. In addition, the cells adsorbed on the zeolite carriers might directly react with the substrate without restrictions on mass transfer, the activity of the adsorbed cells in multiple cyclic reactions is unfavorable and the duration of action and the number of cycles on the zeolites were much lower than for alginate or PVA. The use of alginate microcapsules also was found to be less effective compared to PVA cryogel, since after several cycles of functioning the integrity of the alginate bead shell was completely violated. So, we concluded that the most optimal carrier for immobilizing cells of a consortium of xanthanolytic bacteria was the polyvinyl alcohol cryogel. The PVA cryogel had a strong structure, could stably hold the cell mix creating favorable conditions for their action, which ensured the duration of the process, could be repeatedly used for the biocatalyst without loss of catalytic activity, and had matrix stability.

Testing the capacity of the LE-C1-PVA-cryogel biocatalysts revealed that they were stably functioning with no less than 40 cycles without loss of total xanthanolytic activity, as well as the good properties and stability of the matrix. The total duration of the effective use reached at least 1440 h with an overall xanthanase activity of 20.1 ± 0.6 U/g. The storage of the biocatalyst LE-C1-PVA-cryogel was carried out at temperatures of 4–8 °C in 0.9% NaCl solution. The activity of the biocatalyst was maintained for at least 12 months after storage.

3. Materials and Methods

3.1. Chemicals

Xanthan gum was bought from KondiPro (St. Petersburg, Russia). Chemicals, Luria-Bertrani (LB), Yeast Nitrogen Base without Amino Acids (YNB) media, sugar standards and enzyme substrates (*p*-nitrophenyl β -D-glucopyranoside (pNP β G), *p*-nitrophenyl α -L-mannopyranoside (pNP α M), *p*-nitrophenyl β -D-mannopyranoside (pNP β M) were reagent grade and obtained from Sigma-Aldrich Co. (St. Louis, MO, USA). The *p*-nitrophenyl β -D-thiocellobiopyranoside (pNP β SC) was synthesized according to the method described earlier [60].

3.2. Screening for a Xanthan-Degrading Microorganisms

XP medium containing (g/L) peptone, 1; xanthan, 3; YNB, 0.67, was used for all microbial cultivations. The bacterial xanthan-degrading community was originally derived from the liquid XP medium after maintaining the open vials for 14 days at room temperature. For the enrichment, cultures were incubated in Erlenmeyer flasks (400 mL) containing 100 mL of XP medium at 28 °C for 10 days with aeration using a rotary agitator GFL 3015 (Biotech SL, Madrid, Spain) at 150 rpm. Aliquots of culture liquid were withdrawn periodically for viscosity control and enrichment by spreading a 10-fold serial dilution of the sample on agarized XP and LB plates followed by incubation at 28 °C for 3 days. Isolates were repeatedly tested during the incubation in liquid XP medium for 14 days at 28 °C and aeration at 150 rpm with viscosity control.

The initial bacterial mixture, individual strains KG3 and KG5, as well as the final bacterial consortium LE-C1 were stored at temperatures of 4–8 °C on agarized LB medium (pH 6.5–7.0). Long-term storage of the bacteria under study was carried out in a freeze-dried state in ampoules with a solution containing 10% sucrose and 1% gelatin was used as a cryoprotectant at 4–8 °C in the collection of microorganisms of the Biotechnology Laboratory of the National Research Center “KI” PNPI.

3.3. Genomic Identification

Genomic DNA samples for two potential bacterial isolates were withdrawn from the overnight individual bacterial cultures using a Monarch[®] Genomic DNA Purification Kit (NEB, Ipswich, MA, USA) according to the manufacturer’s protocol. The PCR was carried out with Taq DNA polymerase (Thermo Fisher Scientific, Waltham, MA, USA) and universal

primers 8F and 1492R (l) for the 16S rRNA gene in the Eppendorf Mastercycle Personal. The PCR products were purified with the Cleanup S-Cap kit (Evrogen, Moscow, Russia). The sequencing reactions were carried out with the set of primers (Table 2) and BigDye™ Terminator v3.1 Cycle Sequencing Kit (Thermo Fisher Scientific, Waltham, MA, USA) according to the protocol. The products were purified with the D-Pure™ Dye Terminator Removal kit (Nimagen, Nijmegen, The Netherlands). The electrophoregrams of the purified products were obtained with the Nanophor 05 genetic analyzer (Syntol, Moscow, Russia). Resulting sequences were aligned against the database of 16S ribosomal RNA sequences using the program BLASTN 2.9.0+ [61]. Multiple sequence alignment by ClustalW and phylogenetic analysis were performed using the MEGA X (version 10.1.8) software.

Table 2. Primers used for genomic identification of the isolates.

Primer Name	Primer Sequence	Reference
8F	AGA GTT TGA TCC TGG CTC AG	[62]
357F	CTC CTA CGG GAG GCA GCA G	[62]
CD [R]	CTT GTG CGG GCC CCC GTC AAT TC	[63]
1492R (L)	GGT TAC CTT GTT ACG ACT T	[62]

3.4. Analytic Methods

Viscosities were measured at 22 °C with an LVF Brookfield viscosimeter (Middlesex, London, UK). Protein content was determined by the dye-binding assay of Bradford [64], with bovine serum albumin as a reference protein, measured by light absorption at 595 nm using a JascoV-560 UV/Vis spectrophotometer (Jasco, Analytical Instruments, Tokyo, Japan). The reaction products of xanthan hydrolysis were analyzed by thin layer chromatography (TLC) in the system butanol/acetic acid/water (2:1:1). Cell concentrations were measured by optical density at 650 nm using a calibration curve. The content of cells in 1 mL of culture liquid after the growth of each culture for the calibration curve was determined on the basis of dry weight. All experiments were performed in triplicate.

3.5. Enzyme Assays

The supernatant obtained after the growth of the LE-C1 consortium or individual strains KG3 and KG5 in a liquid XP medium (28 °C, at 150 rpm) by centrifugation (30 min, 3500 rpm) was used for further studies as crude enzyme preparations. Xanthanase activity was determined by measuring reducing sugars using the PAHBAH method [41]. The reaction mixture containing 100 µL of a crude enzyme preparation, 0.3% xanthan solution, and 50 mM sodium citrate–phosphate buffer solution (pH 6.0) was incubated for 2 h at 40 °C. One unit of xanthanase activity was defined as the amount of the enzyme releasing 1 µmol of reducing sugars calculated as glucose, per minute under the assay conditions.

The activities of β-glucosidase, α-mannosidase, β-mannosidase and endo-glucanase/cellulohydrolase were determined using the corresponding chromophoric substrates. The reaction mixture containing 100 µL of a crude enzyme preparation, 5 mM substrate (p-NPβG, p-NPαM, pNPβM, pNPβSC), and 50 mM sodium citrate–phosphate buffer solution (pH 6.0) was incubated for various time periods (not more than 24 h) at 40 °C. The absorption of the released *para*-nitrophenol was measured at 400 nm. One unit of activity was defined as the amount of the enzyme required to produce 1 µmol of *para*-nitrophenol per 1 min under the given conditions.

Xanthan lyase activity was determined in 1 mL of the reaction mixture containing 0.05% xanthan solution and 50 mmol sodium citrate–phosphate buffer solution (pH 6.0), and a crude enzyme preparation, monitoring the increase in absorbance at 235 nm [65]. One unit of enzyme activity was defined as the amount of the enzyme required to increase optical density at 235 nm by 1.0 units per minute.

To determine the optimal pH, xanthanase activity was evaluated by measurement of reducing sugars in a supernatant of the consortium LE-C1 at various pH values using citrate–phosphate (pH 3.0–7.6) and Tris-HCl (pH 8.0–9.0) buffers at 40 °C. To check the pH stability, the samples were preincubated at various pH values (pH 3.0–9.0) at room temperature for 24 h followed by a standard measurement of the activity. The highest activity was taken as 100%.

To determine the temperature optimum for the xanthanase in a supernatant of the consortium LE-C1, enzyme activity was measured at various temperatures (4 °C, 30–60 °C) and pH 6.0. To test the thermostability, the samples of the consortium culture liquid were preincubated at various temperatures and pH 6.0 for 15 min.

3.6. Immobilization of the LE-C1 Consortium

To immobilize the consortium LE-C1 with different techniques, the resulting biomass of each isolate was combined in a ratio of 1:1. Each isolate was preliminarily grown in 1 L Erlenmeyer flask containing 100 mL of a liquid LB medium with aeration at 28 °C at 150 rpm for 24 or 72 h depending on the culture. The cells were centrifuged in the centrifuge 5810 R (Eppendorf, Hamburg, Germany) for 30 min at 3500 rpm, washed with 0.9% (*w/v*) NaCl and centrifuged again under the same conditions. A wet biomass residue with a concentration of $1.6 \div 3.0$ g cell dry weight per L was used for further experiments.

Immobilization on the mineral adsorbent zeolite: zeolite granules with sizes of 0–1 mm, 1–3 mm, and 3–5 mm were used for immobilization. Zeolite granules (12 g) were sterilized by autoclaving for 15 min at 121 °C in distilled water followed by drying, addition of the prepared 10% (*v/v*) of LE-C1 cells prepared as described above, and incubating for 24 h at 4 °C with a Sunflower Mini-Shaker 3D (Biosan SIA, Riga, Latvia) at 40 rpm. Then granules were washed with a solution of 0.9% NaCl until no bacterial cells remained in the washing liquid and stored at 4 °C.

Immobilization in alginate microcapsules: for immobilization of the LE-C1 cells using sodium alginate [66], the 5% solution of sodium alginate in 50 mM Tris-HCl buffer (pH 7.5) was mixed with a 7% (*v/v*) cell suspension prepared as written above. The LE-C1 cell suspension was added with a syringe in small drops to 50 mL of a 0.2 M solution of calcium chloride with constant stirring using the magnetic stirrer MSH-300 (BioSan SIA, Riga, Latvia) at 100 rpm, left for 12 h at 4 °C to form microcapsules, and twice washed with 50 mM Tris-HCl buffer (pH 7.0) at 4 °C. The immobilized whole-cell biocatalyst was stored in Tris-HCl buffer (pH 7.0) at 4 °C until further use.

Immobilization in poly(vinyl alcohol) (PVA): Poly(vinyl alcohol) (12% solution) [67] was dissolved with heating up to 90–100 °C and intensive stirring with the magnetic stirrer at 700 rpm. Prepared LE-C1 bacterial suspensions (4% *v/v*) were thoroughly mixed with 20 mL of cooled PVA solution and aliquoted into a 96-well plate with 200 µL, left at a temperature of –20 °C for 24 h. Then the immobilized whole-cell biocatalyst was stored at 4–8 °C.

To test the capacity of the LE-C1-PVA-cryogel biocatalyst in xanthan depolymerization, it was cultivated at 28 °C and aerated (120 rpm) for 48 h until complete liquefaction of the XP medium. Aliquots of culture liquid were withdrawn periodically for viscosity control. At the end of cultivation, the biocatalyst (cylinders with LE-C1-PVA-cryogel) was removed from the culture liquid with tweezers under sterile conditions, washed with 0.9% NaCl solution, and placed in a new portion of XP medium for the next cycle.

4. Conclusions

Xanthan is a highly stable polysaccharide that most microorganisms, with few exceptions, are unable to depolymerize. The insolubility and highly ordered structure of the polysaccharide are the main problems that should be overcome in order to be accessible to microbial enzyme complexes for its degradation. Obviously, a single microorganism is not always capable of producing the entire pool of enzymes for exhaustive xanthan degradation; so, a consortium of xanthan-degrading microorganisms may be the solution.

In this work, we found a combination of two bacteria in which their enzymatic systems successfully complement each other during the growth of the resulting consortium in a medium containing xanthan until complete depolymerization.

Immobilization of microorganisms is the process of fixing cells on the surface or in the volume of the carrier. The advantages of immobilized cells compared to immobilized enzymes are mainly that they eliminate the most expensive steps of isolation, purification, and immobilization of enzymes. In addition, enzymes in the cell are in their natural environment, which has a positive effect on their thermal stability, as well as stability under conditions of continuous fermentation. There are various methods for immobilizing microbial cells that simplify the extraction and reuse of the catalyst, increase the resistance of cells to lysis, and increase the stability of the enzymatic activity of the immobilized cells and the efficiency of the decomposition process. To the best of our knowledge, the LE-C1 consortium is the first highly stable regenerable biocatalyst immobilized in a poly(vinyl alcohol) matrix for easy and fast use to depolymerize or modify a xanthan polysaccharide.

Author Contributions: A.A.K.: conceptualization, resources, validation, supervision, writing—review and editing. S.V.S.: investigation, writing—original draft. E.V.Z., E.V.E., L.V.Y. and K.S.B.: investigation, validation. All authors have read and agreed to the published version of the manuscript.

Funding: The authors acknowledge financial support from the Genome Research Center Development Program “Kurchatov Genome Center—PNPI” (Agreement No. 075-15-2019-1663).

Data Availability Statement: Not applicable.

Acknowledgments: Authors thank Lubov A. Ivanova for the assistance with Graphical Abstract creation.

Conflicts of Interest: The authors declare no conflict of interest.

References

1. Becker, A.; Katzen, F.; Pühler, A.; Ielpi, L. Xanthan Gum Biosynthesis and Application: A Biochemical/Genetic Perspective. *Appl. Microbiol. Biotechnol.* **1998**, *50*, 145–152. [[CrossRef](#)] [[PubMed](#)]
2. Furtado, I.F.S.P.C.; Sydney, E.B.; Rodrigues, S.A.; Sydney, A.C.N. Xanthan Gum: Applications, Challenges, and Advantages of This Asset of Biotechnological Origin. *Biotechnol. Res. Innov.* **2022**, *6*, e202204. [[CrossRef](#)]
3. More, T.T.; Yadav, J.S.S.; Yan, S.; Tyagi, R.D.; Surampalli, R.Y. Extracellular Polymeric Substances of Bacteria and Their Potential Environmental Applications. *J. Environ. Manag.* **2014**, *144*, 1–25. [[CrossRef](#)]
4. Wu, M.; Qu, J.; Tian, X.; Zhao, X.; Shen, Y.; Shi, Z.; Chen, P.; Li, G.; Ma, T. Tailor-Made Polysaccharides Containing Uniformly Distributed Repeating Units Based on the Xanthan Gum Skeleton. *Int. J. Biol. Macromol.* **2019**, *131*, 646–653. [[CrossRef](#)] [[PubMed](#)]
5. Bhat, I.M.; Wani, S.M.; Mir, S.A.; Masoodi, F.A. Advances in Xanthan Gum Production, Modifications and Its Applications. *Biocatal. Agric. Biotechnol.* **2022**, *42*, 102328. [[CrossRef](#)]
6. Carvalho, L.T.; Vieira, T.A.; Zhao, Y.; Celli, A.; Medeiros, S.F.; Lacerda, T.M. Recent Advances in the Production of Biomedical Systems Based on Polyhydroxyalkanoates and Exopolysaccharides. *Int. J. Biol. Macromol.* **2021**, *183*, 1514–1539. [[CrossRef](#)]
7. BeMiller, J.N. *Carbohydrate Chemistry for Food Scientists*, 3rd ed.; Elsevier Inc.: Philadelphia, PA, USA; Woodhead Publishing: Cambridge, UK; AACC International Press: St. Paul, MN, USA, 2018; Volume 11, pp. 261–269.
8. Kool, M.M.; Gruppen, H.; Sworn, G.; Schols, H.A. The Influence of the Six Constituent Xanthan Repeating Units on the Order–Disorder Transition of Xanthan. *Carbohydr. Polym.* **2014**, *104*, 94–100. [[CrossRef](#)]
9. Riaz, T.; Iqbal, M.W.; Jiang, B.; Chen, J. A Review of the Enzymatic, Physical, and Chemical Modification Techniques of Xanthan Gum. *Int. J. Biol. Macromol.* **2021**, *186*, 472–489. [[CrossRef](#)]
10. Palaniraj, A.; Jayaraman, V. Production, Recovery and Applications of Xanthan Gum by *Xanthomonas campestris*. *J. Food Eng.* **2011**, *106*, 1–12. [[CrossRef](#)]
11. Nsengiyumva, E.M.; Alexandridis, P. Xanthan Gum in Aqueous Solutions: Fundamentals and Applications. *Int. J. Biol. Macromol.* **2022**, *216*, 583–604. [[CrossRef](#)] [[PubMed](#)]
12. Bagnol, R.; Grijpma, D.; Eglin, D.; Moriarty, T.F. The Production and Application of Bacterial Exopolysaccharides as Biomaterials for Bone Regeneration. *Carbohydr. Polym.* **2022**, *291*, 119550. [[CrossRef](#)]
13. Han, G.; Chen, Q.; Liu, F.; Cui, Z.; Shao, H.; Liu, F.; Ma, A.; Liao, J.; Guo, B.; Guo, Y. Low Molecular Weight Xanthan Gum for Treating Osteoarthritis. *Carbohydr. Polym.* **2017**, *164*, 386–395. [[CrossRef](#)]
14. Chen, Q.; Shao, X.; Ling, P.; Liu, F.; Shao, H.; Ma, A.; Wu, J.; Zhang, W.; Liu, F.; Han, G. Low Molecular Weight Xanthan Gum Suppresses Oxidative Stress-Induced Apoptosis in Rabbit Chondrocytes. *Carbohydr. Polym.* **2017**, *169*, 255–263. [[CrossRef](#)] [[PubMed](#)]
15. Yuan, F.; Xie, J.-L.; Liu, K.-Y.; Shan, J.-L.; Sun, Y.-G.; Ying, W.-G. Xanthan Gum Protects Temporomandibular Chondrocytes from IL-1 β through Pin1/NF- κ B Signaling Pathway. *Mol. Med. Rep.* **2020**, *22*, 1129–1136. [[CrossRef](#)] [[PubMed](#)]

16. Zhang, W.; Wu, J.; Zhang, F.; Dou, X.; Ma, A.; Zhang, X.; Shao, H.; Zhao, S.; Ling, P.; Liu, F. Lower Range of Molecular Weight of Xanthan Gum Inhibits Apoptosis of Chondrocytes through MAPK Signaling Pathways. *Int. J. Biol. Macromol.* **2019**, *130*, 79–87. [[CrossRef](#)]
17. Shao, X.; Chen, Q.; Dou, X.; Chen, L.; Wu, J.; Zhang, W.; Shao, H.; Ling, P.; Liu, F.; Wang, F. Lower Range of Molecular Weight of Xanthan Gum Inhibits Cartilage Matrix Destruction via Intrinsic Bax-Mitochondria Cytochrome c-Caspase Pathway. *Carbohydr. Polym.* **2018**, *198*, 354–363. [[CrossRef](#)]
18. Sun, L.; Zhang, Z.; Leng, K.; Li, B.; Feng, C.; Huo, X. Can Supramolecular Polymers Become Another Material Choice for Polymer Flooding to Enhance Oil Recovery? *Polymers* **2022**, *14*, 4405. [[CrossRef](#)] [[PubMed](#)]
19. Christensen, B.E.; Smidsroed, O.; Elgsaeter, A.; Stokke, B.T. Depolymerization of Double-Stranded Xanthan by Acid Hydrolysis: Characterization of Partially Degraded Double Strands and Single-Stranded Oligomers Released from the Ordered Structures. *Macromolecules* **1993**, *26*, 6111–6120. [[CrossRef](#)]
20. Cheetham, N.W.H.; Mashimba, E.N.M. Characterisation of Some Enzymic Hydrolysis Products of Xanthan. *Carbohydr. Polym.* **1991**, *15*, 195–206. [[CrossRef](#)]
21. Christensen, B.E.; Smidsrød, O. Dependence of the Content of Unsubstituted (Cellulosic) Regions in Prehydrolysed Xanthans on the Rate of Hydrolysis by *Trichoderma reesei* Endoglucanase. *Int. J. Biol. Macromol.* **1996**, *18*, 93–99. [[CrossRef](#)]
22. Yang, F.; Li, H.; Sun, J.; Guo, X.; Zhang, X.; Tao, M.; Chen, X.; Li, X. Novel Endotype Xanthanase from Xanthan-Degrading *Microbacterium* sp. Strain XT11. *Appl. Environ. Microbiol.* **2019**, *85*, e01800-18. [[CrossRef](#)] [[PubMed](#)]
23. Nankai, H.; Hashimoto, W.; Miki, H.; Kawai, S.; Murata, K. Microbial System for Polysaccharide Depolymerization: Enzymatic Route for Xanthan Depolymerization by *Bacillus* sp. Strain GL1. *Appl. Environ. Microbiol.* **1999**, *65*, 2520–2526. [[CrossRef](#)]
24. Ashraf, S.; Soudi, M.R.; Amoozegar, M.A.; Moshtaghi Nikou, M.; Spröer, C. *Paenibacillus xanthanilyticus* sp. nov., a Xanthan-Degrading Bacterium Isolated from Soil. *Int. J. Syst. Evol. Microbiol.* **2018**, *68*, 76–80. [[CrossRef](#)]
25. Muchová, M.; Růžička, J.; Julínová, M.; Doležalová, M.; Houser, J.; Koutný, M.; Buňková, L. Xanthan and Gellan Degradation by Bacteria of Activated Sludge. *Water Sci. Technol.* **2009**, *60*, 965–973. [[CrossRef](#)] [[PubMed](#)]
26. Ashraf, S.; Soudi, M.R.; Ghadam, P. Production of Xanthanases by *Paenibacillus* spp.: Complete Xanthan Degradation and Possible Applications. *Iran. J. Biotechnol.* **2017**, *15*, 120–127. [[CrossRef](#)] [[PubMed](#)]
27. Cadmus, M.C.; Jackson, L.K.; Burton, K.A.; Plattner, R.D.; Slodki, M.E. Biodegradation of Xanthan Gum by *Bacillus* sp. *Appl. Environ. Microbiol.* **1982**, *44*, 5–11. [[CrossRef](#)] [[PubMed](#)]
28. Ruijsenaars, H.J.; de Bont, J.A.; Hartmans, S. A Pyruvated Mannose-Specific Xanthan Lyase Involved in Xanthan Degradation by *Paenibacillus alginolyticus* XL-1. *Appl. Environ. Microbiol.* **1999**, *65*, 2446–2452. [[CrossRef](#)]
29. Ruijsenaars, H.J.; Hartmans, S.; Verdoes, J.C. A Novel Gene Encoding Xanthan Lyase of *Paenibacillus alginolyticus* Strain XL-1. *Appl. Environ. Microbiol.* **2000**, *66*, 3945–3950. [[CrossRef](#)]
30. Liu, H.; Huang, C.; Dong, W.; Du, Y.; Bai, X.; Li, X. Biodegradation of Xanthan by Newly Isolated *Cellulomonas* Sp. LX, Releasing Elicitor-Active Xantho-Oligosaccharides-Induced Phytoalexin Synthesis in Soybean Cotyledons. *Process Biochem.* **2005**, *40*, 3701–3706. [[CrossRef](#)]
31. Qian, F.; An, L.; Wang, M.; Li, C.; Li, X. Isolation and Characterization of a Xanthan-Degrading *Microbacterium* sp. Strain XT11 from Garden Soil. *J. Appl. Microbiol.* **2007**, *102*, 1362–1371. [[CrossRef](#)]
32. Hu, X.; Wang, K.; Yu, M.; He, P.; Qiao, H.; Zhang, H.; Wang, Z. Characterization and Antioxidant Activity of a Low-Molecular-Weight Xanthan Gum. *Biomolecules* **2019**, *9*, 730. [[CrossRef](#)]
33. Kool, M.M.; Gruppen, H.; Sworn, G.; Schols, H.A. Comparison of Xanthans by the Relative Abundance of Its Six Constituent Repeating Units. *Carbohydr. Polym.* **2013**, *98*, 914–921. [[CrossRef](#)] [[PubMed](#)]
34. Cadmus, M.C.; Slodki, M.E.; Nicholson, J.J. High-Temperature, Salt-Tolerant Xanthanase. *J. Ind. Microbiol.* **1989**, *4*, 127–133. [[CrossRef](#)]
35. Hou, C.T.; Barnabe, N.; Greaney, K. Biodegradation of Xanthan by Salt-Tolerant Aerobic Microorganisms. *J. Ind. Microbiol.* **1986**, *1*, 31–37. [[CrossRef](#)]
36. Martins, S.C.S.; Martins, C.M.; Fiúza, L.M.C.G.; Santaella, S.T. Immobilization of Microbial Cells: A Promising Tool for Treatment of Toxic Pollutants in Industrial Wastewater. *Afr. J. Biotechnol.* **2013**, *12*, 4412–4418. [[CrossRef](#)]
37. Yang, P.Y.; Cai, T.; Wang, M.-L. Immobilized Mixed Microbial Cells for Wastewater Treatment. *Biol. Wastes* **1988**, *23*, 295–312. [[CrossRef](#)]
38. Abdul Manaf, S.A.; Mohamad Fuzi, S.F.Z.; Abdul Manas, N.H.; Md Illias, R.; Low, K.O.; Hegde, G.; Che Man, R.; Wan Azelee, N.I.; Matias-Peralta, H.M. Emergence of Nanomaterials as Potential Immobilization Supports for Whole Cell Biocatalysts and Cell Toxicity Effects. *Biotechnol. Appl. Biochem.* **2021**, *68*, 1128–1138. [[CrossRef](#)]
39. Zhang, J.; Wei, J.; Massey, I.Y.; Peng, T.; Yang, F. Immobilization of Microbes for Biodegradation of Microcystins: A Mini Review. *Toxins* **2022**, *14*, 573. [[CrossRef](#)] [[PubMed](#)]
40. Polakovič, M.; Švitel, J.; Bučko, M.; Filip, J.; Neděla, V.; Ansoerge-Schumacher, M.B.; Gemeiner, P. Progress in Biocatalysis with Immobilized Viable Whole Cells: Systems Development, Reaction Engineering and Applications. *Biotechnol. Lett.* **2017**, *39*, 667–683. [[CrossRef](#)]
41. Mühlmann, M.; Kunze, M.; Ribeiro, J.; Geinitz, B.; Lehmann, C.; Schwaneberg, U.; Commandeur, U.; Büchs, J. Cellulolytic RoboLector—Towards an Automated High-Throughput Screening Platform for Recombinant Cellulase Expression. *J. Biol. Eng.* **2017**, *11*, 1. [[CrossRef](#)]

42. Tamura, K.; Peterson, D.; Peterson, N.; Stecher, G.; Nei, M.; Kumar, S. MEGA5: Molecular Evolutionary Genetics Analysis Using Maximum Likelihood, Evolutionary Distance, and Maximum Parsimony Methods. *Mol. Biol. Evol.* **2011**, *28*, 2731–2739. [[CrossRef](#)]
43. Kumar, S.; Stecher, G.; Li, M.; Knyaz, C.; Tamura, K. MEGA X: Molecular Evolutionary Genetics Analysis across Computing Platforms. *Mol. Biol. Evol.* **2018**, *35*, 1547–1549. [[CrossRef](#)]
44. Jensen, P.F.; Kadziola, A.; Comamala, G.; Segura, D.R.; Anderson, L.; Poulsen, J.-C.N.; Rasmussen, K.K.; Agarwal, S.; Sainathan, R.K.; Monrad, R.N.; et al. Structure and Dynamics of a Promiscuous Xanthan Lyase from *Paenibacillus nanensis* and the Design of Variants with Increased Stability and Activity. *Cell Chem. Biol.* **2019**, *26*, 191–202.e6. [[CrossRef](#)] [[PubMed](#)]
45. Dasman; Kajiyama, S.; Okazawa, A.; Fukusaki, E.; Kobayashi, A. Purification and Properties of an Enzyme Capable of Degrading the Polysaccharide of the Cyanobacterium, *Nostoc commune*. *Z. Naturforschung C J. Biosci.* **2002**, *57*, 1042–1046. [[CrossRef](#)] [[PubMed](#)]
46. Fu, Y.; Cheng, L.; Meng, Y.; Li, S.; Zhao, X.; Du, Y.; Yin, H. *Cellulosimicrobium cellulans* Strain E4-5 Enzymatic Hydrolysis of Curdlan for Production of (1→3)-Linked β -D-Glucan Oligosaccharides. *Carbohydr. Polym.* **2015**, *134*, 740–744. [[CrossRef](#)]
47. Dou, T.-Y.; Chen, J.; Hao, Y.-F.; Qi, X. Xylanosomes Produced by *Cellulosimicrobium cellulans* F16 Were Diverse in Size, but Resembled in Subunit Composition. *Arch. Microbiol.* **2019**, *201*, 163–170. [[CrossRef](#)] [[PubMed](#)]
48. Vu, N.T.-H.; Quach, T.N.; Dao, X.T.-T.; Le, H.T.; Le, C.P.; Nguyen, L.T.; Le, L.T.; Ngo, C.C.; Hoang, H.; Chu, H.H.; et al. A Genomic Perspective on the Potential of Termite-Associated *Cellulosimicrobium cellulans* MP1 as Producer of Plant Biomass-Acting Enzymes and Exopolysaccharides. *PeerJ* **2021**, *9*, e11839. [[CrossRef](#)]
49. Kool, M.M.; Schols, H.A.; Delahaije, R.J.B.M.; Sworn, G.; Wierenga, P.A.; Gruppen, H. The Influence of the Primary and Secondary Xanthan Structure on the Enzymatic Hydrolysis of the Xanthan Backbone. *Carbohydr. Polym.* **2013**, *97*, 368–375. [[CrossRef](#)] [[PubMed](#)]
50. Chhabra, S.R.; Shockley, K.R.; Connors, S.B.; Scott, K.L.; Wolfinger, R.D.; Kelly, R.M. Carbohydrate-Induced Differential Gene Expression Patterns in the Hyperthermophilic Bacterium *Thermotoga maritima*. *J. Biol. Chem.* **2003**, *278*, 7540–7552. [[CrossRef](#)]
51. Emami Moghaddam, S.A.; Harun, R.; Mokhtar, M.N.; Zakaria, R. Potential of Zeolite and Algae in Biomass Immobilization. *BioMed Res. Int.* **2018**, *2018*, 6563196. [[CrossRef](#)]
52. Wang, S.; Peng, Y. Natural Zeolites as Effective Adsorbents in Water and Wastewater Treatment. *Chem. Eng. J.* **2010**, *156*, 11–24. [[CrossRef](#)]
53. Mery, C.; Guerrero, L.; Alonso-Gutiérrez, J.; Figueroa, M.; Lema, J.M.; Montalvo, S.; Borja, R. Evaluation of Natural Zeolite as Microorganism Support Medium in Nitrifying Batch Reactors: Influence of Zeolite Particle Size. *J. Environ. Sci. Health Part A Toxic/Hazard. Subst. Environ. Eng.* **2012**, *47*, 420–427. [[CrossRef](#)]
54. Kubota, M.; Nakabayashi, T.; Matsumoto, Y.; Shiomi, T.; Yamada, Y.; Ino, K.; Yamanokuchi, H.; Matsui, M.; Tsunoda, T.; Mizukami, F.; et al. Selective Adsorption of Bacterial Cells onto Zeolites. *Colloids Surf. B Biointerfaces* **2008**, *64*, 88–97. [[CrossRef](#)]
55. Smidsrod, O.; Skjåk-Braek, G. Alginate as Immobilization Matrix for Cells. *Trends Biotechnol.* **1990**, *8*, 71–78. [[CrossRef](#)]
56. Lozinsky, V.I. Polymeric Cryogels as a New Family of Macroporous and Supermacroporous Materials for Biotechnological Purposes. *Russ. Chem. Bull.* **2008**, *57*, 1015–1032. [[CrossRef](#)]
57. Berillo, D.; Al-Jwaid, A.; Caplin, J. Polymeric Materials Used for Immobilisation of Bacteria for the Bioremediation of Contaminants in Water. *Polymers* **2021**, *13*, 1073. [[CrossRef](#)] [[PubMed](#)]
58. Razavi, M.; Qiao, Y.; Thakor, A.S. Three-Dimensional Cryogels for Biomedical Applications. *J. Biomed. Mater. Res. A* **2019**, *107*, 2736–2755. [[CrossRef](#)]
59. Plieva, F.M.; Galaev, I.Y.; Noppe, W.; Mattiasson, B. Cryogel Applications in Microbiology. *Trends Microbiol.* **2008**, *16*, 543–551. [[CrossRef](#)]
60. Ibatullin, F.; Selivanov, S.; Shavva, A. A General Procedure for Conversion of S-Glycosyl Isothiourea Derivatives into Thioglycosides, Thiooligosaccharides and Glycosyl Thioesters. *Synthesis* **2001**, *2001*, 0419–0422. [[CrossRef](#)]
61. Zhang, Z.; Schwartz, S.; Wagner, L.; Miller, W. A Greedy Algorithm for Aligning DNA Sequences. *J. Comput. Biol. J. Comput. Mol. Cell Biol.* **2000**, *7*, 203–214. [[CrossRef](#)]
62. Turner, S.; Pryer, K.M.; Miao, V.P.; Palmer, J.D. Investigating Deep Phylogenetic Relationships among Cyanobacteria and Plastids by Small Subunit rRNA Sequence Analysis. *J. Eukaryot. Microbiol.* **1999**, *46*, 327–338. [[CrossRef](#)] [[PubMed](#)]
63. Rudi, K.; Skulberg, O.M.; Larsen, F.; Jakobsen, K.S. Strain Characterization and Classification of Oxyphotobacteria in Clone Cultures on the Basis of 16S rRNA Sequences from the Variable Regions V6, V7, and V8. *Appl. Environ. Microbiol.* **1997**, *63*, 2593–2599. [[CrossRef](#)] [[PubMed](#)]
64. Bradford, M.M. A Rapid and Sensitive Method for the Quantitation of Microgram Quantities of Protein Utilizing the Principle of Protein-Dye Binding. *Anal. Biochem.* **1976**, *72*, 248–254. [[CrossRef](#)]
65. Hashimoto, W.; Miki, H.; Tsuchiya, N.; Nankai, H.; Murata, K. Xanthan Lyase of *Bacillus* sp. Strain GL1 Liberates Pyruvylated Mannose from Xanthan Side Chains. *Appl. Environ. Microbiol.* **1998**, *64*, 3765–3768. [[CrossRef](#)]

66. Gür, S.D.; İdil, N.; Aksöz, N. Optimization of Enzyme Co-Immobilization with Sodium Alginate and Glutaraldehyde-Activated Chitosan Beads. *Appl. Biochem. Biotechnol.* **2018**, *184*, 538–552. [[CrossRef](#)]
67. Stepanov, N.; Efremenko, E. “Deceived” Concentrated Immobilized Cells as Biocatalyst for Intensive Bacterial Cellulose Production from Various Sources. *Catalysts* **2018**, *8*, 33. [[CrossRef](#)]

Disclaimer/Publisher’s Note: The statements, opinions and data contained in all publications are solely those of the individual author(s) and contributor(s) and not of MDPI and/or the editor(s). MDPI and/or the editor(s) disclaim responsibility for any injury to people or property resulting from any ideas, methods, instructions or products referred to in the content.